Eur. Phys. J. C (2022) 82:1055
https://doi.org/10.1140/epjc/s10052-022-10994-7

THE EUROPEAN PHYSICAL JOURNAL C

Regular Article - Theoretical Physics

pp scattering at the LHC with the lepton pair production and one proton tagging

S. I. Godunov[1], **E. K. Karkaryan**[1], **V. A. Novikov**[1], **A. N. Rozanov**[2], **M. I. Vysotsky**[1], **E. V. Zhemchugov**[1,a]

[1] I. E. Tamm Department of Theoretical Physics, Lebedev Physical Institute, 53 Leninskiy Prospekt, Moscow 119991, Russia
[2] Centre de Physique de Particules de Marseille (CPPM), Aux-Marseille Universite, CNRS/IN2P3, 163 avenue de Luminy, case 902, 13288 Marseille, France

Received: 7 September 2022 / Accepted: 1 November 2022 / Published online: 22 November 2022

Abstract Analytical formulas for the cross section of the reaction $pp \to p + \ell^+\ell^- + X$ are presented. Fiducial cross sections are compared with those measured recently by the ATLAS collaboration.

1 Introduction

Lepton pairs produced in ultraperipheral collisions (UPC) of protons at the Large Hadron Collider (LHC) are accompanied by forward scattering of the protons. Previous measurements of this process were performed by the ATLAS collaboration without proton tagging [1]. We have calculated the cross section for this reaction with the help of the equivalent photon approximation (EPA) in [2], taking into account the so-called survival factor which addresses the diminishing of the cross section because of proton disintegration due to strong interactions. The result obtained agrees with the measurement within the experimental accuracy. Predictions for the cross section were also made with the help of Monte-Carlo calculations [3–6].

The CMS and TOTEM collaborations have reported statistically significant proton-tagged dilepton production [7], but the cross sections have not been measured. The ATLAS collaboration has managed to measure the cross sections [8]. In the events selected for the analysis, one of the scattered protons is detected by the ATLAS Forward Proton Spectrometer. The other proton could remain intact, in which case it could or could not be detected by the opposite forward detector, or it could disintegrate. The transversal momentum of the lepton pair $p_T^{\ell\ell}$ was required to be less than 5 GeV. This momentum equals to the sum of transversal momenta of the photons emitted by the protons. The transversal momentum of the photon that was emitted by the proton that survived the collision cannot be much higher than $\hat{q} = 0.2$ GeV [9]. Therefore, the transversal momentum of the second photon has to be less than 5 GeV.

In what follows we derive analytical formulas which describe the fiducial cross sections measured in [8]. These formulas allow for simple numerical integration instead of the usual Monte Carlo approach and thus can provide intuitive insights into the process targeted by the experiment. Our numerical results are in the ballpark of experimental data, while their substantial deviation would signal New Physics. This paper is a continuation of the work presented in our previous paper [10] where we have derived formulas for the cross section without experimental cuts on the leptons phase space and with no requirement for any of the protons to hit the forward detectors.

In Sect. 2 we calculate the fiducial cross section for the case of elastic scattering of the second proton. The contribution to the fiducial cross section of the processes when the second proton disintegrates is calculated in Sect. 3. We conclude in Sect. 4.

2 Fiducial cross section for the reaction $pp \to p + \ell^+\ell^- + p$

The spectrum of photons radiated by proton is [9]

$$n_p(\omega) = \frac{2\alpha}{\pi\omega} \int_0^\infty \frac{D(Q^2)}{Q^4} q_\perp^3 \, \mathrm{d}q_\perp, \tag{1}$$

where α is the fine structure constant, $Q^2 \equiv -q^2 = q_\perp^2 + \omega^2/\gamma^2$, q is the photon 4-momentum, $q_\perp$ is the photon transverse momentum, ω is the photon energy, $\gamma = E_p/m_p \approx 6.93 \cdot 10^3$ is the Lorentz factor of the proton, $E_p = 6.5$ TeV

[a] e-mail: zhemchugovev@lebedev.ru (corresponding author)

is the proton energy, m_p is the proton mass,[1]

$$D(Q^2) = \frac{G_E^2(Q^2) + \frac{Q^2}{4m_p^2} G_M^2(Q^2)}{1 + \frac{Q^2}{4m_p^2}}, \tag{2}$$

$G_E(Q^2)$ and $G_M(Q^2)$ are the Sachs electric and magnetic form factors. For the Sachs form factors we use the dipole approximation:

$$G_E(Q^2) = \frac{1}{(1+Q^2/\Lambda^2)^2}, \; G_M(Q^2) = \frac{\mu_p}{(1+Q^2/\Lambda^2)^2},$$
$$\Lambda^2 = \frac{12}{r_p^2} = 0.66 \text{ GeV}^2, \tag{3}$$

where $\mu_p = 2.79$ is the proton magnetic moment, and $r_p = 0.84$ fm is the proton charge radius [11]. Substituting (2), (3) into (1), we obtain the following analytical expression:

$$\begin{aligned} n_p(\omega) = \frac{\alpha}{\pi\omega} \Bigg\{ & \left(1 + 4u - (\mu_p^2 - 1)\frac{u}{v}\right) \ln\left(1 + \frac{1}{u}\right) \\ & - \frac{24u^2 + 42u + 17}{6(u+1)^2} - \frac{\mu_p^2 - 1}{(v-1)^3} \Bigg[\frac{1+u/v}{v-1} \ln \frac{u+v}{u+1} \\ & - \frac{6u^2(v^2 - 3v + 3) + 3u(3v^2 - 9v + 10) + 2v^2 - 7v + 11}{6(u+1)^2} \Bigg] \Bigg\}, \end{aligned} \tag{4}$$

where

$$u = \left(\frac{\omega}{\Lambda\gamma}\right)^2, \; v = \left(\frac{2m_p}{\Lambda}\right)^2. \tag{5}$$

The cross section for the lepton pair production in the case when both of the protons survive is

$$\sigma(pp \to p + \ell^+\ell^- + p) = \int_0^\infty \int_0^\infty \sigma(\gamma\gamma \to \ell^+\ell^-)\, n_p(\omega_1)\, n_p(\omega_2)\, \mathrm{d}\omega_1\, \mathrm{d}\omega_2, \tag{6}$$

where $\sigma(\gamma\gamma \to \ell^+\ell^-)$ is the cross section for the production of a lepton pair in a collision of two real photons with energies ω_1 and ω_2. The plus signs in the reaction notation indicate large rapidity gaps between the produced particles.

In [8], as well as in all other measurements made at the LHC, the phase space is constrained by the following requirements: $p_{i,T} > \hat{p}_T$, $|\eta_i| < \hat{\eta}$, where $p_{i,T}$ is the transversal momentum of lepton ℓ_i, and η_i is its pseudorapidity. In the case of muons $\hat{p}_T = 15$ GeV and $\hat{\eta} = 2.4$, while in the case of electrons $\hat{p}_T = 18$ GeV and $\hat{\eta} = 2.47$. The transversal momentum of the lepton pair is equal to the sum of the transversal momenta of the photons and is limited by $\sqrt{Q^2} \lesssim \hat{q} = 0.2$ GeV, so transversal momenta of the leptons are equal with good accuracy: $p_T \equiv p_{1,T} \approx p_{2,T}$.

[1] In Ref. [9], the Dirac form factor squared was used instead of $D(Q^2)$. It leads to incorrect accounting for the magnetic form factor.

Neglecting the lepton mass, the differential fiducial cross section in this case is

$$\frac{\mathrm{d}\sigma_{\text{fid.}}(pp \to p + \ell^+\ell^- + p)}{\mathrm{d}W} = \int_{\max\left(\hat{p}_T, \frac{W}{2\cosh\hat{\eta}}\right)}^{W/2} \mathrm{d}p_T \frac{\mathrm{d}\sigma(\gamma\gamma \to \ell^+\ell^-)}{\mathrm{d}p_T} \frac{\mathrm{d}\hat{L}}{\mathrm{d}W}, \tag{7}$$

where $W = \sqrt{4\omega_1\omega_2}$ is the invariant mass of the lepton pair,

$$\frac{\mathrm{d}\sigma(\gamma\gamma \to \ell^+\ell^-)}{\mathrm{d}p_T} = \frac{8\pi\alpha^2}{W^2 p_T} \cdot \frac{1 - 2p_T^2/W^2}{\sqrt{1 - 4p_T^2/W^2}} \tag{8}$$

[12], $\mathrm{d}\hat{L}/\mathrm{d}W$ is the photon–photon luminosity taking into account the limits on the phase space,

$$\frac{\mathrm{d}\hat{L}}{\mathrm{d}W} = \frac{W}{2} \int_{-\hat{y}}^{\hat{y}} n_p\left(\tfrac{W}{2}\mathrm{e}^y\right) n_p\left(\tfrac{W}{2}\mathrm{e}^{-y}\right) \mathrm{d}y, \tag{9}$$

$y = \frac{1}{2}\ln\frac{\omega_1}{\omega_2}$ is the rapidity of the lepton pair, and the integration over ω_1 and ω_2 in (6) is changed to the integration over W and y: $\mathrm{d}\omega_1\mathrm{d}\omega_2 = \frac{W}{2}\mathrm{d}W\mathrm{d}y$. The pseudorapidities of charged leptons for given values of W and p_T are determined by the value of y. In this way the cut on η $(-\hat{\eta} < \eta < \hat{\eta})$ is transformed to the cut on y: $-\hat{y} < y < \hat{y}$, where [9, (B.9)][2]

$$\hat{y} = \hat{\eta} + \frac{1}{2}\ln\frac{1 - \sqrt{1 - 4p_T^2/W^2}}{1 + \sqrt{1 - 4p_T^2/W^2}}. \tag{10}$$

Here $\hat{y}$ has to be greater than zero; this requirement leads to the inequality $p_T > \frac{W}{2\cosh\hat{\eta}}$ in the lower limit of the integration with respect to p_T in (7).

Another requirement imposed in [8] is that one of the protons hits the forward detector. To do that, the proton must lose a fraction of its energy ξ: $\xi_{\min} < \xi < \xi_{\max}$, where $\xi_{\min} = 0.035$, $\xi_{\max} = 0.08$. This translates to limits on the energy of the photon emitted by this proton:

$$227 \text{ GeV} \equiv \omega_{\min} < \omega_1 < \omega_{\max} \equiv 520 \text{ GeV}. \tag{11}$$

To take that into account, the integration limits in eq. (9) have to be narrowed:

$$\frac{\mathrm{d}\hat{L}_{\text{FD}}}{\mathrm{d}W} = \frac{W}{2} \int_{\max(-\hat{y},\tilde{y})}^{\min(\hat{y},\tilde{Y})} n_p\left(\tfrac{W}{2}\mathrm{e}^y\right) n_p\left(\tfrac{W}{2}\mathrm{e}^{-y}\right) \mathrm{d}y, \tag{12}$$

[2] Reference [9] uses $x = \omega_1/\omega_2 \equiv \mathrm{e}^{2y}$.

where FD stands for the “forward detector”,

$$\tilde{y} = \ln \max\left(\frac{2\omega_{1,\min}}{W}, \frac{W}{2\omega_{2,\max}}\right),$$
$$\tilde{Y} = \ln \min\left(\frac{2\omega_{1,\max}}{W}, \frac{W}{2\omega_{2,\min}}\right), \tag{13}$$

$\omega_{1,\min}, \omega_{1,\max}, \omega_{2,\min}, \omega_{2,\max}$ are the limits on energy losses for each of the protons.[3] Calculation with

$$\omega_{1,\min} = \omega_{\min}, \quad \omega_{2,\min} = 0,$$
$$\omega_{1,\max} = \omega_{\max}, \quad \omega_{2,\max} = \infty \tag{14}$$

will result in the fiducial cross section with the first proton hitting the forward detector. Calculation with

$$\omega_{1,\min} = \omega_{\min}, \quad \omega_{2,\min} = \omega_{\min},$$
$$\omega_{1,\max} = \omega_{\max}, \quad \omega_{2,\max} = \omega_{\max} \tag{15}$$

yields the fiducial cross section with both protons hitting the forward detectors. To calculate the cross section measured in [8], one has to multiply the former by 2 and subtract the latter to avoid double counting:

$$\sigma_{\text{fid.,[8]}}(pp \to p + \ell^+\ell^- + p)$$
$$= 2\sigma_{\text{fid}}(pp \to p + \ell^+\ell^- + p)|_{(14)} - \sigma_{\text{fid}}(pp \to p$$
$$+\ell^+\ell^- + p)|_{(15)}. \tag{16}$$

In both measurements in [8], the selected region of invariant masses of lepton pairs was $W > 20$ GeV with the region 70 GeV $< W <$ 105 GeV excluded to suppress the background from Z decays. Collecting together all of the phase space constraints relevant to the exclusive process (see Ref. [94] in [8]), we get:

- 20 GeV $< W <$ 70 GeV or $W >$ 105 GeV.
- $0.035 < \xi < 0.08$ which is equivalent to 227 GeV $< \omega <$ 520 GeV.
- For muons:
  - $\hat{p}_T = 15$ GeV, $\hat{\eta} = 2.4$.
  - $\sigma_{\text{fid.,[8]}}(pp \to p + \mu^+\mu^- + p) = 8.6$ fb.
- For electrons:
  - $\hat{p}_T = 18$ GeV, $\hat{\eta} = 2.47$.
  - $\sigma_{\text{fid.,[8]}}(pp \to p + e^+e^- + p) = 10.1$ fb.

[3] This change may result in poor numerical convergence of the integral with respect to p_T in (7) when $\tilde{y}$ and $\tilde{Y}$ have the same sign. To address that, the lower integration limit in (7) should be replaced with $\max\left(\hat{p}_T, \frac{W}{2\cosh\hat{\eta}}, \frac{W}{2\cosh(\max(\tilde{y}, -\tilde{Y}) - \hat{\eta})}\right)$.

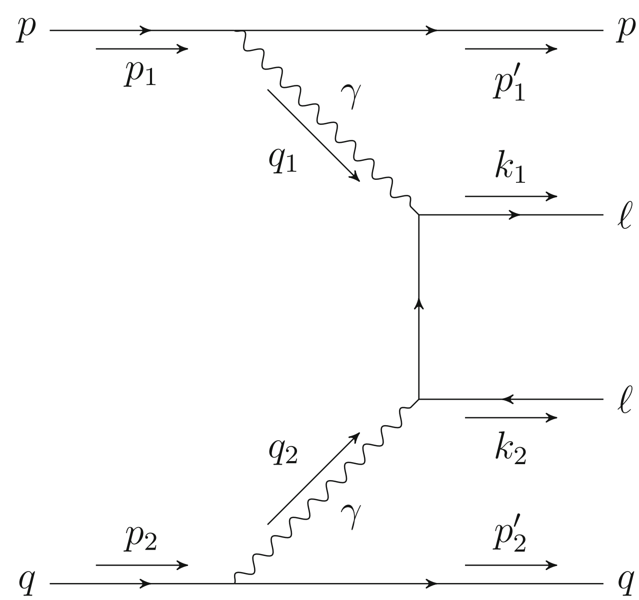

Fig. 1 Lepton pair production in semiexclusive reaction

3 Fiducial cross section for the reaction $pp \to p + \ell^+\ell^- + X$

In this section we calculate the cross section for lepton pair production with one of the protons scattered elastically and detected by the forward detector, while the other proton disintegrates. Following the parton model, we consider this process as a two-photon lepton pair production in a collision of a proton and a quark, summed over all quarks:

$$\sigma(pp \to p + \ell^+\ell^- + X)$$
$$= \sum_q \sigma(pq \to p + \ell^+\ell^- + q). \tag{17}$$

One of the Feynman diagrams of the $pq \to p + \ell^+\ell^- + q$ reaction is presented in Fig. 1.

In the laboratory system we have the following expressions for the momenta of the colliding particles:

$$p_1 = (E, 0, 0, E), \ \ p_2 = (xE, 0, 0, -xE), \tag{18}$$

where x is the fraction of the momentum of the disintegrating proton carried by the quark. In the following we will integrate over x from a value much less than 1 to 1, but the numerically important values of x are of the order of 1/3, so we have neglected here the masses of the proton m_p and the quark m_q: $E/m_p = \gamma \approx 6.93 \cdot 10^3 \gg 1$, $xE/m_q \gg 1$ even for the (sea) b quark.

The momentum of the photon emitted by the proton,

$$q_1 = \left(\omega_1, \vec{\mathbf{q}}_{1\perp}, \frac{\omega_1\gamma}{\sqrt{\gamma^2 - 1}}\right), \tag{19}$$

where $\vec{\mathbf{q}}_{1\perp}$ is its transversal momentum. The 4-momentum squared,

$$Q_1^2 \equiv -q_1^2 \approx q_{1\perp}^2 + (\omega_1/\gamma)^2, \tag{20}$$

is limited by the condition that the proton survives: $Q_1^2 \lesssim \hat{q}^2 \approx (0.2\text{ GeV})^2$ [9], so the first photon is approximately real: $Q_1^2 \ll W^2$. Therefore, the equivalent photon approximation can be used here.

For the second photon, we also apply the equivalent photon approximation, but with a correction.[4] Since the quark is bound within the proton, we use the constituent quark mass $m_q = m_p/3 \approx 300$ MeV to describe its properties.[5] The momentum of the second photon

$$q_2 \approx \left(\omega_2, \vec{\mathbf{q}}_{2\perp}, -\frac{\omega_2\gamma_q}{\sqrt{\gamma_q^2-1}}\right), \tag{21}$$

and its square is

$$Q_2^2 \equiv -q_2^2 \approx q_{2\perp}^2 + (\omega_2/\gamma_q)^2, \tag{22}$$

where $\gamma_q = E_q/m_q = 3xE_p/m_p = 3x\gamma$. In the ATLAS measurement the following upper bound was effectively imposed on $q_{2\perp}$: $|\vec{\mathbf{q}}_{1\perp} + \vec{\mathbf{q}}_{2\perp}| \sim q_{2\perp} < \hat{p}_T^{\ell\ell} = 5$ GeV.

The square of the invariant mass of the lepton pair $W^2 = (q_1+q_2)^2 \approx 2q_1q_2 + q_2^2 \approx 4\omega_1\omega_2 - Q_2^2$. For $W \sim 100$ GeV, $Q_2^2 \ll W^2$, and $\omega_2 \approx W^2/4\omega_1$. Here ω_1 is bounded by the requirement that the proton hits the forward detector (11). Therefore, ω_2 is of the order of a few GeV — the lepton pair will have large rapidity towards the detector that registers the proton. We assume $\omega_1 \ll E$ and $\omega_2 \ll xE$ in the following.

To derive the cross section for the $pq \to p + \ell^+\ell^- + q$ reaction, we follow closely Ref. [14] and begin with its Eq. (5.1) (multiplied by the parton distribution function $f_q(x, Q_2^2)$):

$$\begin{aligned} &d\sigma(pq \to p + \ell^+\ell^- + q) \\ &= \frac{Q_q^2(4\pi\alpha)^2}{q_1^2q_2^2}\rho_1^{\mu\nu}\rho_2^{\alpha\beta}M_{\mu\alpha}M_{\nu\beta}^* \\ &\times \frac{(2\pi)^4\delta^{(4)}(q_1+q_2-k_1-k_2)d\Gamma}{4\sqrt{(p_1p_2)^2 - p_1^2p_2^2}} \\ &\times \frac{d^3p_1'}{(2\pi)^3 2E_1'}\frac{d^3p_2'}{(2\pi)^3 2E_2'} \times f_q(x, Q_2^2)dx, \end{aligned} \tag{23}$$

where Q_q is the electric charge of quark q, $\rho_1^{\mu\nu}$ and $\rho_2^{\alpha\beta}$ are the photon density matrices for the photons emitted by the proton or the quark respectively, $M_{\mu\alpha}$ is the amplitude for the $\gamma^*\gamma^* \to \ell^+\ell^-$ process, $d\Gamma$ is the phase space element of the lepton pair, E_1' and E_2' are the energies of the proton and the quark after the collision.

Since $p_i' = p_i - q_i$, we rewrite the phase space element of the proton and the quark as follows:

$$\frac{d^3p_1'}{E_1'}\cdot\frac{d^3p_2'}{E_2'} \approx \frac{d^2q_{1\perp}d\omega_1}{E}\cdot\frac{d^2q_{2\perp}d\omega_2}{xE}. \tag{24}$$

The photon density matrix for the photon emitted by the proton is

$$\begin{aligned} \rho_1^{\mu\nu} &= -\frac{1}{2q_1^2}\,\mathrm{Tr}\left\{(\hat{p}_1' + m_p)\left(F_1(Q_1^2)\gamma^\mu + F_2(Q_1^2)\frac{\sigma^{\mu\alpha}q_1^\alpha}{2m_p}\right)\right. \\ &\left.\times(\hat{p}_1 + m_p)\left(F_1(Q_1^2)\gamma^\nu - F_2(Q_1^2)\frac{\sigma^{\nu\alpha}q_1^\alpha}{2m_p}\right)\right\}, \end{aligned} \tag{25}$$

where $F_1(Q_1^2)$ and $F_2(Q_1^2)$ are the Dirac and Pauli form factors. The Sachs form factors (3) are their linear combinations:

$$\begin{aligned} G_E(Q_1^2) &= F_1(Q_1^2) - \frac{Q_1^2}{4m_p^2}F_2(Q_1^2), \\ G_M(Q_1^2) &= F_1(Q_1^2) + F_2(Q_1^2). \end{aligned} \tag{26}$$

Equation (25) simplifies to

$$\begin{aligned} \rho_1^{\mu\nu} &= -\left(g^{\mu\nu} - \frac{q_1^\mu q_1^\nu}{q_1^2}\right)G_M^2(Q_1^2) \\ &\quad - \frac{(2p_1-q_1)^\mu(2p_1-q_1)^\nu}{q_1^2}D(Q_1^2), \end{aligned} \tag{27}$$

where $D(Q_1^2)$ is defined in Eq. (2).

The photon density matrix for the photon emitted by the quark is

$$\begin{aligned} \rho_2^{\mu\nu} &= -\frac{1}{2q_2^2}\,\mathrm{Tr}\left\{\hat{p}_2'\gamma^\mu\hat{p}_2\gamma^\nu\right\} = -\left(g^{\mu\nu} - \frac{q_2^\mu q_2^\nu}{q_2^2}\right) \\ &\quad - \frac{(2p_2-q_2)^\mu(2p_2-q_2)^\nu}{q_2^2}. \end{aligned} \tag{28}$$

It is convenient to consider the lepton pair production in the basis of virtual photon helicity states. In the center of mass system of the colliding photons, let $q_1 = (\tilde{\omega}_1, 0, 0, \tilde{q})$, $q_2 = (\tilde{\omega}_2, 0, 0, -\tilde{q})$. The standard set of orthonormal 4-vectors orthogonal to q_1 and q_2 is

$$\begin{aligned} e_1^+ &= \frac{1}{\sqrt{2}}(0,-1,-i,0),\; e_1^- = \frac{1}{\sqrt{2}}(0,1,-i,0), \\ e_1^0 &= \frac{i}{\sqrt{-q_1^2}}(\tilde{q},0,0,\tilde{\omega}_1), \\ e_2^+ &= \frac{1}{\sqrt{2}}(0,1,-i,0),\; e_2^- = \frac{1}{\sqrt{2}}(0,-1,-i,0), \\ e_2^0 &= \frac{i}{\sqrt{-q_2^2}}(-\tilde{q},0,0,\tilde{\omega}_2). \end{aligned} \tag{29}$$

[4] Another option would be to use the parton distribution for photons, see for example [13].

[5] Variation of m_q from 200 to 400 MeV changes the values of the cross sections presented in Eqs. (45), (46) by less than 1%. It is clear that at the present level of experimental accuracy the uncertainty due to the choice of the quark mass is negligible.

Due to the conservation of vector current, the covariant density matrices $\rho_i^{\mu\nu}$ satisfy $q_1^\mu \rho_1^{\mu\nu} = q_2^\mu \rho_2^{\mu\nu} = 0$. Thus, we can write

$$\rho_i^{\mu\nu} = \sum_{a,b} (e_i^{a\mu})^* e_i^{b\nu} \rho_i^{ab}, \tag{30}$$

$$\rho_i^{ab} = (-1)^{a+b} e_i^{a\mu} (e_i^{b\nu})^* \rho_i^{\mu\nu}, \tag{31}$$

where $a, b \in \{\pm 1, 0\}$, and ρ_i^{ab} are the density matrices in the helicity representation. The amplitudes of the lepton pair production in the helicity basis M_{ab} comply to the equation

$$\rho_1^{\mu\nu} \rho_2^{\alpha\beta} M_{\mu\alpha} M_{\nu\beta}^* = (-1)^{a+b+c+d} \rho_1^{ab} \rho_2^{cd} M_{ac} M_{bd}^*. \tag{32}$$

In this expression, non-diagonal terms (those with $a \neq b$ or $c \neq d$) originate from the interference and cancel out when integrated over azimuthal angles of the proton and the quark in the final state [14,15]. Contributions to the cross section for lepton pair production by longitudinally polarized photons are proportional to $Q_1^2/W^2 \leq \hat{q}^2/W^2 \ll 1$ and $Q_2^2/W^2 \leq (p_T^{\ell\ell})^2/W^2 \ll 1$ and are neglected in the following. Thus, we can rewrite (23) in the helicity representation:

$$\begin{aligned} &\mathrm{d}\sigma(pq \to p + \ell^+\ell^- + q) \\ &= Q_q^2 (4\pi\alpha)^2 \Big(\rho_1^{++}\rho_2^{++}|M_{++}|^2 + \rho_1^{++}\rho_2^{--}|M_{+-}|^2 \\ &\quad + \rho_1^{--}\rho_2^{++}|M_{-+}|^2 + \rho_1^{--}\rho_2^{--}|M_{--}|^2\Big) \\ &\quad \times \frac{(2\pi)^4 \delta^{(4)}(q_1 + q_2 - k_1 - k_2)\mathrm{d}\Gamma}{4 p_1 p_2} \\ &\quad \times \frac{\mathrm{d}^2 q_{1\perp} \mathrm{d}\omega_1}{(2\pi)^3 q_1^2 E} \cdot \frac{\mathrm{d}^2 q_{2\perp} \mathrm{d}\omega_2}{(2\pi)^3 q_2^2 x E} \cdot f_q(x, Q_2^2)\mathrm{d}x. \end{aligned} \tag{33}$$

Substitution of (27), (28) to (31) yields the following expressions

$$\begin{aligned} &\rho_1^{++} = \rho_1^{--} = G_M^2(Q_1^2) + \frac{2p_{1\perp}^2}{q_1^2} D(Q_1^2), \\ &\rho_2^{++} = \rho_2^{--} = 1 + \frac{2p_{2\perp}^2}{q_2^2}, \end{aligned} \tag{34}$$

where $p_{i\perp}$ is the component of the momentum p_i orthogonal to q_i in the c.m.s. of the colliding photons. To calculate it, we follow [14] and introduce the symmetrical tensor

$$\begin{aligned} &R^{\mu\nu}(q_1, q_2) = -g^{\mu\nu} \\ &+ \frac{q_1 q_2 \cdot (q_1^\mu q_2^\nu + q_1^\nu q_2^\mu) - q_1^2 q_2^\mu q_2^\nu - q_2^2 q_1^\mu q_1^\nu}{(q_1 q_2)^2 - q_1^2 q_2^2}. \end{aligned} \tag{35}$$

This tensor is the metric tensor of the subspace orthogonal to q_1 and q_2, and has the following properties:

$$q_i^\mu R^{\mu\nu} = 0, \;\; R^{\alpha\beta} R^{\beta\gamma} = -R^{\alpha\gamma}, \;\; R^{\alpha\beta} R^{\alpha\beta} = 2. \tag{36}$$

Then $p_{i,\perp}^\mu = -R^{\mu\nu} p_i^\nu$, and[6]

$$\begin{aligned} &\rho_1^{++} = \rho_1^{--} = G_M^2(Q_1^2) \\ &\quad + D(Q_1^2)\left[\frac{2m_p^2}{q_1^2} + \frac{1}{2}\left(\frac{(2p_1 q_2 - q_1 q_2)^2}{(q_1 q_2)^2 - q_1^2 q_2^2} - 1\right)\right], \\ &\rho_2^{++} = \rho_2^{--} = \frac{1}{2} + \frac{2m_q^2}{q_2^2} + \frac{1}{2} \cdot \frac{(2p_2 q_1 - q_1 q_2)^2}{(q_1 q_2)^2 - q_1^2 q_2^2}. \end{aligned} \tag{37}$$

With the help of Eqs. (18)–(22), under the assumptions $q_1^2 q_2^2 \ll (q_1 q_2)^2$, $\omega_1 \ll E$, $\omega_2 \ll xE$, these expressions simplify to

$$\begin{aligned} \rho_1^{++} = \rho_1^{--} &\approx G_M^2(Q_1^2) + 2D(Q_1^2)\left[\frac{m_p^2}{q_1^2} + \left(\frac{E}{\omega_1}\right)^2\right] \\ &\approx D(Q_1^2) \cdot \frac{2E^2 q_{1\perp}^2}{\omega_1^2 Q_1^2}, \\ \rho_2^{++} = \rho_2^{--} &\approx 1 + 2\left[\frac{m_q^2}{q_2^2} + \left(\frac{xE}{\omega_2}\right)^2\right] \approx \frac{2x^2 E^2 q_{2\perp}^2}{\omega_2^2 Q_2^2}. \end{aligned} \tag{38}$$

Substitution of Eqs. (38) to (33) yields

$$\begin{aligned} &\mathrm{d}\sigma(pq \to p + \ell^+\ell^- + q) \approx \left(\frac{2Q_q \alpha}{\pi}\right)^2 \\ &\frac{q_1 q_2}{p_1 p_2} x E^2 \sigma(\gamma\gamma \to \ell^+\ell^-) D(Q_1^2) \frac{q_{1\perp}^3 \mathrm{d}q_{1\perp}}{Q_1^4} \frac{\mathrm{d}\omega_1}{\omega_1^2} \\ &\times \frac{q_{2\perp}^3 \mathrm{d}q_{2\perp}}{Q_2^4} \frac{\mathrm{d}\omega_2}{\omega_2^2} \cdot f_q(x, Q_2^2)\mathrm{d}x, \end{aligned} \tag{39}$$

where

$$\begin{aligned} &\sigma(\gamma\gamma \to \ell^+\ell^-) = \int \frac{1}{4}[|M_{++}|^2 + |M_{+-}|^2 \\ &\quad + |M_{-+}|^2 + |M_{--}|^2] \frac{(2\pi)^4 \delta^{(4)}(q_1 + q_2 - k_1 - k_2)\mathrm{d}\Gamma}{4 q_1 q_2}, \end{aligned} \tag{40}$$

is the cross for lepton pair production in a collision of two real unpolarized photons. Integration over $q_{1\perp}$ yields the equivalent photon spectrum of proton (1). To derive the fiducial cross section, we change the integration variables: $\mathrm{d}\omega_1 \mathrm{d}\omega_2 = \frac{W}{2}\mathrm{d}W\mathrm{d}y$. Then

$$\begin{aligned} &\mathrm{d}\sigma(pq \to p + \ell^+\ell^- + q) \approx \frac{2Q_q^2 \alpha}{\pi} \, n_p\left(\frac{W}{2}\mathrm{e}^y\right) \\ &\sigma(\gamma\gamma \to \ell^+\ell^-)\, \mathrm{e}^y \, \frac{q_{2\perp}^3 \mathrm{d}q_{2\perp}}{Q_2^4} \mathrm{d}W\mathrm{d}y \; f_q(x, Q_2^2)\mathrm{d}x. \end{aligned} \tag{41}$$

[6] The identity $q_1^2 = 2p_1 q_1$ helps in deriving Eq. (37).

Introducing the function

$$n_q(\omega) = \frac{2Q_q^2\alpha}{\pi\omega}\int\limits_{\omega/E}^{1} \mathrm{d}x \int\limits_0^{p_T^{\ell\ell}} \mathrm{d}q_{2\perp}\, \frac{q_{2\perp}^3}{Q_2^4} f_q(x, Q_2^2), \tag{42}$$

which can be loosely interpreted as the equivalent photon spectrum of quark q (cf. (1)), we derive the equation for the fiducial cross section similar to (7), (12):

$$\frac{\mathrm{d}\sigma_{\text{fid.}}(pp \to p + \ell^+\ell^- + X)}{\mathrm{d}W} = \sum_q \int\limits_{\max\left(\hat{p}_T,\, \frac{W}{2\cosh\tilde{\eta}}\right)}^{W/2} \mathrm{d}p_T \frac{\mathrm{d}\sigma(\gamma\gamma \to \ell^+\ell^-)}{\mathrm{d}p_T} \times \frac{W}{2} \int\limits_{\max(-\hat{y},\tilde{y})}^{\min(\hat{y},\tilde{Y})} \mathrm{d}y\, n_p\left(\frac{W}{2}e^y\right) n_q\left(\frac{W}{2}e^{-y}\right). \tag{43}$$

Similar to (16), to calculate the cross section measured in [8], this value should be multiplied by 2 to take into account that either of the protons can hit the detector:

$$\sigma_{\text{fid.,[8]}}(pp \to p + \ell^+\ell^- + X) = 2\sigma_{\text{fid.,[8]}}(pp \to p + \ell^+\ell^- + X). \tag{44}$$

Using the parton distribution functions `MSHT20nnlo_as118` [16] provided by the LHAPDF [17] library, we get the cross sections

$$\sigma_{\text{fid.,[8]}}(pp \to p + \mu^+\mu^- + X) = 9.6 \text{ fb}, \tag{45}$$
$$\sigma_{\text{fid.,[8]}}(pp \to p + e^+e^- + X) = 11.4 \text{ fb}. \tag{46}$$

In order to estimate the accuracy of these cross sections, we have calculated them with the shifted arguments of parton density functions:

$$f_q(x, Q_2^2/2): \quad \begin{cases} \sigma(pp \to p + \mu^+\mu^- + X) = 7.7 \text{ fb}, \\ \sigma(pp \to p + e^+e^- + X) = 9.1 \text{ fb}, \end{cases} \tag{47}$$

$$f_q(x, 2Q_2^2): \quad \begin{cases} \sigma(pp \to p + \mu^+\mu^- + X) = 11.5 \text{ fb}, \\ \sigma(pp \to p + e^+e^- + X) = 13.6 \text{ fb}. \end{cases} \tag{48}$$

We have checked that the contribution from the region of small Q^2 where the PDFs are known with less accuracy is small. To do that we have calculated the inelastic contribution with much stronger cut on the transverse momentum: $Q^2 \approx q_\perp^2 < 1$ GeV^2. We get 2.2 fb for the production of muons and 2.6 fb for the production of electrons. Therefore, it is about 20% of the inelastic contribution, and of the order of what we have estimated for the PDFs uncertainty. We add this as a separate source of the uncertainty of the inelastic contribution.

We must also stress here that PDFs alone do not describe all inelastic contribution and there is a contribution to proton structure functions from resonance phenomena and other effects, see [13,18,19]. From Figure 18 of Ref. [13] and Table I of Ref. [18] we can see that the contribution of these effects is non-vanishing but at the level of 10–15% from elastic contribution. We do not aim at such level of precision and take into account just major contributions.

4 Conclusions

Let us compare our results with experimental data from [8]:

$$\sigma^{\text{exp.}}_{\mu\mu+p} = 7.2 \pm 1.6 \text{ (stat.)} \pm 0.9 \text{ (syst.)} \pm 0.2 \text{ (lumi.) fb}, \tag{49}$$

$$\sigma^{\text{exp.}}_{ee+p} = 11.0 \pm 2.6 \text{ (stat.)} \pm 1.2 \text{ (syst.)} \pm 0.3 \text{ (lumi.) fb}. \tag{50}$$

Summing up the cross sections calculated in Sects. 2 and 3, we get:

$$\tilde{\sigma}^{\text{theor.}}_{\mu\mu+p} = 18 \pm 3 \text{ fb}, \tag{51}$$
$$\tilde{\sigma}^{\text{theor.}}_{ee+p} = 22 \pm 3 \text{ fb}, \tag{52}$$

where the uncertainty values were obtained by comparing Eqs. (47), (48) and (45), (46) and include the uncertainty of the contribution from the region of small Q^2, see the paragraph after (48). Also was taken into account the very small contribution from quark mass uncertainty in (21), see footnote 5 at page 4.

The so-called survival factor takes into account the diminishing of the cross sections due to breaking of both protons occurring when the protons scatter with small impact parameter b. The survival factor decreases when the invariant mass of the lepton pair grows and for the elastic cross section at $W \sim 100$ GeV it approximately equals to 0.9 according to Fig. 3 from [2].

Table 1 in [8] contains results for the cross section obtained by Monte Carlo simulation. From the first two lines of this Table it follows that the survival factor (the probability for the colliding protons to avoid strong interactions) decreases the cross section by approximately factor 1.5. Here the values of cross sections for $S_{\text{surv}} = 1$ are the combined results of LPAIR and HERWIG event generators, and the results for the survival factor from papers [5,6] are used. Results of SUPERCHIC4 code [20] which takes the survival factor into account are within one standard deviation, see the third line in Table 1.

In the case of the elastic process, according to [2] the cross section is approximately 10% less, while in the case of elastic-inelastic scattering the cross section is approximately 50% less, see the lower left panel of Fig. 28 from Ref. [18].

We see that when the survival factor is taken into account the derived formulae are in agreement with experimental data at the level of 2–3 standard deviations. In the case of elastic process, the survival factor is calculated in [2] and can be easily taken into account without resorting to Monte Carlo simulations. Whether calculations of survival factor for semiexclusive process can be performed in a similar way is an interesting subject for further study.

Monte Carlo codes for photon–photon processes in UPC of protons and/or nuclei are presented in the recent paper [21].

Our calculations were performed with the help of `libepa` [22].

We are grateful to the referee for emphasizing the necessity of analysis of the contribution of low Q^2 domain to the inelastic cross section.

Funding Funding was provided by Russian Science Foundation (19-12-00123-П).

Data Availability Statement This manuscript has no associated data or the data will not be deposited. [Authors' comment: No data was generated and no unpublished data was used in the course of this work.]

References

1. The ATLAS Collaboration, Measurement of the exclusive $\gamma\gamma \to \mu^+\mu^-$ process in proton–proton collisions at $\sqrt{s} = 13$ TeV with the ATLAS detector. Phys. Lett. B **777**, 303 (2018). https://doi.org/10.1016/j.physletb.2017.12.043. arXiv:1708.04053
2. S.I. Godunov, V.A. Novikov, A.N. Rozanov, M.I. Vysotsky, E.V. Zhemchugov, Production of heavy charged particles in proton–proton ultraperipheral collisions at the Large Hadron Collider: survival factor. JHEP **2021**, 234 (2021). https://doi.org/10.1007/JHEP10(2021)234. arXiv:2106.14842
3. M. Bähr, S. Gieseke, M.A. Gigg, D. Grellscheid et al., Herwig++ physics and manual. Eur. Phys. J. C **58**, 639 (2008). https://doi.org/10.1140/epjc/s10052-008-0798-9. arXiv:0803.0883
4. J. Bellm, S. Gieseke, D. Grellscheid, S. Plätzer et al., Herwig 7.0/Herwig++ 3.0 release note. Eur. Phys. J. **C76**, 196 (2016). https://doi.org/10.1140/epjc/s10052-016-4018-8. arXiv:1512.01178
5. M. Dyndal, L. Schoeffel, The role of finite-size effects on the spectrum of equivalent photons in proton–proton collisions at the LHC. Phys. Lett. B **741**, 66 (2015). https://doi.org/10.1016/j.physletb.2014.12.019. arXiv:1410.2983
6. L.A. Harland-Lang, V.A. Khoze, M.G. Ryskin, Exclusive physics at the LHC with SuperChic 2. Eur. Phys. J. C **76**, 9 (2016). https://doi.org/10.1140/epjc/s10052-015-3832-8. arXiv:1508.02718
7. The CMS and TOTEM collaborations, Observation of proton-tagged, central (semi)exclusive production of high-mass lepton pairs in pp collisions at 13 TeV with the CMS-TOTEM precision proton spectrometer. JHEP 2018, 153 (2018). https://doi.org/10.1007/JHEP07(2018)153. arXiv:1803.04496
8. The ATLAS collaboration, Observation and measurement of forward proton scattering in association with lepton pairs produced via the photon fusion mechanism at ATLAS. Phys. Rev. Lett. **125**, 261801 (2020). https://doi.org/10.1103/PhysRevLett.125.261801. arXiv:2009.14537
9. M. Vysotsky, E. Zhemchugov, Equivalent photons in proton–proton and ion-ion collisions at the Large Hadron Collider. Phys. Uspekhi **62**, 910 (2019). https://doi.org/10.3367/UFNe.2018.07.038389. arXiv:1806.07238
10. S. I. Godunov, E.K. Karkaryan, V.A. Novikov, A.N. Rozanov, M.I. Vysotsky, E.V. Zhemchugov. Forward proton scattering in association with muon pair production via the photon fusion mechanism at the LHC. JETP Lett. **115**, 59 (2022). https://doi.org/10.1134/S0021364022020011. arXiv:2112.01870
11. E. Tiesinga, P.J. Mohr, D.B. Newell, B.N. Taylor. CODATA recommended values of the fundamental physical constants: 2018. Rev. Mod. Phys. **93**, 025010 (2021). https://doi.org/10.1103/RevModPhys.93.025010
12. V.B. Beresteckii, E.M. Lifshitz, L.P. Pitaevskii. Kvantovaya Elektrodynamika (Fizmatlit, Moscow, 2001),
13. A.V. Manohar, P. Nason, G.P. Salam, G. Zanderighi, The photon content of the proton. JHEP **2017**, 46 (2017). https://doi.org/10.1007/JHEP12(2017)046. arXiv:1708.01256
14. V.M. Budnev, I.F. Ginzburg, G.V. Meledin, V.G. Serbo, The two-photon particle production mechanism. Physical problems, applications, equivalent photon approximation. Phys. Rep. **15**, 181 (1974). https://doi.org/10.1016/0370-1573(75)90009-5
15. A. Dobrovolskaya, V. Novikov, On heavy Higgs boson production. Z. Phys. C **52**, 427 (1991). https://doi.org/10.1007/BF01559437
16. S. Bailey, T. Cridge, L.A. Harland-Lang, A.D. Martin, R.S. Thorne, Parton distributions from LHC, HERA, Tevatron and fixed target data: MSHT20 PDFs. Eur. Phys. J. C **81**, 341 (2021). https://doi.org/10.1140/epjc/s10052-021-09057-0. arXiv:2012.04684
17. A. Buckley, J. Ferrando, S. Lloyd, K. Nordström, B. Page, M. Rüefenacht, M. Schönherr, G. Watt, LHAPDF6: parton density access in the LHC precision era. Eur. Phys. J. C **75**, 132 (2015). https://doi.org/10.1140/epjc/s10052-015-3318-8. arXiv:1412.7420
18. A. Szczurek, B. Linek, M. Łuszczak, Semiexclusive dilepton production in proton–proton collisions with one forward proton measurement at the LHC. Phys. Rev. D **104**, 074009 (2021). https://doi.org/10.1103/PhysRevD.104.074009. arXiv:2107.02535
19. M. Łuszczak, W. Schäfer, A. Szczurek, Two-photon dilepton production in proton–proton collisions: two alternative approaches. Phys. Rev. D **93**, 074018 (2016). https://doi.org/10.1103/PhysRevD.93.074018. arXiv:1510.00294
20. L.A. Harland-Lang, M. Tasevsky, V.A. Khoze, M.G. Ryskin, A new approach to modelling elastic and inelastic photon-initiated production at the LHC: SuperChic 4. Eur. Phys. J. C **80**, 925 (2020). https://doi.org/10.1140/epjc/s10052-020-08455-0 arXiv:2007.12704

21. H.-S. Shao, D. d'Enterria, gamma-UPC: Automated generation of exclusive photon–photon processes in ultraperipheral proton and nuclear collisions with varying form factors. JHEP **2022**, 248 (2022). https://doi.org/10.1007/JHEP09(2022)248 arXiv:2207.03012
22. `libepa`: library for calculations of cross sections of ultraperipheral collisions of high energy particles under the equivalent photons approximation. https://github.com/jini-zh/libepa